IOP Conf. Series: Materials Science and Engineering **1344** (2026) 012065 doi:10.1088/1757-899X/1344/1/012065

Development of a simulation code for analysing pressure and temperature fluctuations in the J-PARC cryogenic moderator system

H Tatsumoto[1*], G Ariyoshi[2], M Teshigawara[2]

[1] European Spallation Source (ESS) ERIC, Lund, Sweden.
[2] Japan Atomic Energy Agency, Tokai, Japan.

*E-mail: hideki.tatsumoto@ess.eu

Abstract. At the J-PARC spallation neutron source, a cryogenic moderator system (CMS) was designed to circulate supercritical hydrogen at 162 g/s, removing a transient heat load of 3.8 kW during 1-MW proton beam operation while limiting the temperature rise below 3 K. A parallel flow configuration for moderator distribution lines was adopted to ensure consistent delivery of 18 K hydrogen to each moderator. The CMS is cooled by a helium refrigerator with a cooling capacity of 6.4 kW at 16 K. In this study, a comprehensive simulation code was developed that incorporates the parallel distribution lines and heat exchanger to estimate the propagation of temperature fluctuations throughout the entire CMS loop and the impact on the return helium temperature to the refrigerator. The simulation results demonstrated good agreement with measured data, validating the model's ability to accurately predict temperature propagation across the CMS loop.

1. Introduction

At the Japan Proton Accelerator Research Complex (J-PARC), 3-GeV proton beams (1 MW), generated by an accelerator, strikes a mercury target at a rate of 25 Hz, producing fast neutrons through a spallation reaction [1]. These high-energy neutrons are moderated to produce cold neutrons suitable for neutron scattering experiments by passing through three types of hydrogen moderators: a coupled moderator (CM) for high intensity, a poisoned moderator (PM) for sharp pulse shape, and a decoupled moderator (DM) that provides a balance between intensity and pulse sharpness. The moderatos operate using supercritical hydrogen at 1.5 MPa and 18 K [2]. During 1-MW proton beam operation, nuclear heating in the hydrogen moderator is estimated to be 3.8 kW. The cryogenic moderator system (CMS) circulates supercritical hydrogen at a flow rate of 162 g/s to remove this transient heat load and limit the temperature rise below 3 K, as shown in Fig. 1 [2]. A parallel configuration of 22 m-long transfer lines ensures the consistent delivery of hydrogen at 18 K to each moderator. The CMS is cooled by a helium refrigerator with a cooling capacity of 6.4 kW at 16 K, utilizing a plate-fin type heat exchanger [3]. An ortho-to-parahydrogen catalyst vessel is integrated to maintain parahydrogen fraction exceeding 99%. Additionally, a pressure mitigation system was developed to mitigate pressure fluctuations caused by transient temperature rises in the moderators. This system consists of a heater and an accumulator with helium-filled bellows, ensuring stable operation during proton beam injection or trip events [4,5].

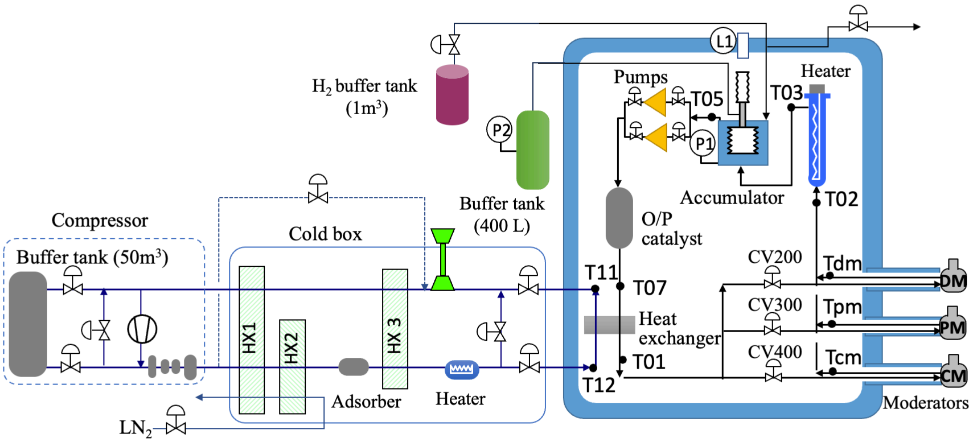

Figure 1. Overview of the J-PARC cryogenic moderator system (CMS).

Tatsumoto et al. [6] developed a simplified simulation model to study the cooldown process of the J-PARC CMS and optimize operational parameters. In this model, the parallel distribution lines to the moderators were treated as a combined single line, and the removal heat load was directly applied, without modeling the heat exchanger. However, as the proton beam power increases, it becomes necessary to adjust the flow distribution to ensure that the temperature rise across the moderators remains below 3 K.

In this study, we developed a new simulation code to optimize the J-PARC CMS operational conditions for the current 1-MW and the planned future 1.5-MW proton beam operations at the upgrade target station. This code builds on the previous cool-down simulation model [6] and a heat exchanger model [7, 8]. The new code incorporates the parallel distribution lines and heat exchanger to estimate the propagation of temperature fluctuations throughout the entire CMS loop and the resulting temperature fluctuations in the helium flow returning to the refrigerator cold box. The simulation model is validated data under the off-beam conditions.

2. Simulation model

2.1 Analytical model

Figure 2 shows a one-dimensional analytical model that considers only the hydrogen loop. In this model, the process pipe is primarily made of stainless steel, except for the moderator vessel, which is constructed from aluminum alloy. The three transfer lines are arranged in parallel. The two hydrogen pumps, also arranged in parallel, are simplified into a single combined pump. The main loop has an outer diameter of 42.7 mm and a wall thickness of 2.0 mm. The total hydrogen inventory is estimated to be 206.4 L, including the bellows with a volume of 61 liters and a variable volume of 6.84 liters at the intermediate position [2]. Helium gas, which behaves as a compressible fluid at approximately 20 K, is enclosed in the bellows at a pressure of 1.55 MPa. The bellows are connected to a buffer tank with a volume of 400 liters at room temperature

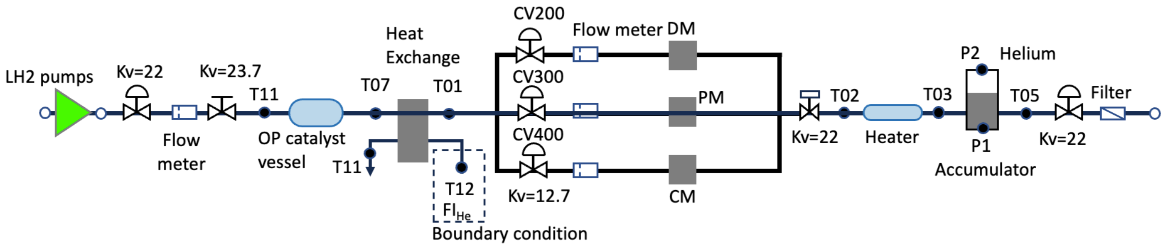

Figure 2. Simulation model.

through a 20-m long pipe with a volume of 9.5 liters. The ortho-para hydrogen catalyst vessel contains a catalyst packed-bed volume of 35 liters, filled with 32% porous hydrous ferric oxide catalyst. The Kv value of the flow control valve for the moderator is 15.3, while the Kv value at the inlet of the catalyst vessel is 25.6. For the other control valves, the Kv value is 21.9. The orifice flow meters, located in the moderator transfer lines and at the pump outlet, have betas of 0.624 and 0.502, respectively. The heat exchanger model [8] is integrated into this analytical model to simulate the propagation of temperature fluctuations downstream of the heat exchanger and the resulting return helium temperature. In the analytical model, the hydrogen loop is represented as a one-dimensional pipe with a cross-sectional area of 1.1 $\times 10^{-3}$ m^2, and divided into 2638 grids. Each grid has a volume of 7.83 $\times 10^{-5}$ m^3. In the heat exchange model, a helium cooling channel is modelled and divided into 93 grids with a volume of 7.83 $\times 10^{-5}$ m^3.

2.2 Basic equations

2.2.1 Combined hydrogen pump characteristics

Gas bearing-type pumps [9] are arranged in parallel upstream the catalyst vessel and the heat exchanger. Each pump features a closed impeller with a diameter, D, of 26.0 mm. These pumps are capable of operating at revolution speed, N, ranging from 30,000 to 63,000 rpm, with an allowable pump head of up to 120 kPa. The performance can be described using dimensionless expressions of the head coefficient, ψ, and the discharge coefficient, ϕ. The performance curve of the combined hydrogen pump is expressed using the dimensionless parameters as follows [6, 9].

$$\psi = \frac{\Delta P}{\rho {u_S}^2} \tag{1}$$

$$\phi = \frac{\dot{m}}{\rho u_S D^2} \tag{2}$$

where $u_s = \pi ND/60$ is the wheel speed, ρ is the density, $\dot{m}$ is the discharge mass flow, u_s is the wheel speed and ΔP is the pump head.

The heat load generated by the pump, Q_p, is calculated by the following correlation.

$$Q_p = \frac{\dot{m}\Delta P}{\rho\eta} \tag{3}$$

where η is the adiabatic pump efficiency, which is set to 0.5 [6, 9].

2.2.2 Enthalpy equation

Heat transport through the hydrogen loop is calculated using the following enthalpy equation. The diffusion term in the enthalpy equation is ignored in the analysis and expressed as follows:

$$\frac{\partial(\rho h)}{\partial t} = -\frac{\partial(\rho u h)}{\partial x} + \frac{\partial}{\partial x}\left(\lambda\frac{\partial T}{\partial x}\right) + S \tag{4}$$

where h is the enthalpy, u is the flow velocity, λ is the thermal conductivity and S is the energy source.

2.2.3 Pressure drop calculations

IOP Conf. Series: Materials Science and Engineering **1344** (2026) 012065 doi:10.1088/1757-899X/1344/1/012065

The pressure drop through the pipe, ΔP, is calculated using a friction factor determined by the Colebrook equation [10] with a surface roughness, ε, of 0.05 mm.

$$\frac{1}{\sqrt{f}} = -2log\left(\frac{\varepsilon}{3.7d_H} + \frac{2.51}{Re\sqrt{f}}\right) \tag{5}$$

where f is the friction factor, Re is the Reynolds number and d_H is the hydraulic diameter.

The hydrogen transfer lines features a coaxial corrugated pipe structure composed of five layers: hydrogen supply piping, a vacuum insulation layer, hydrogen return piping, another vacuum insulation layer, and an outer helium blanket layer. The friction factor for the corrugated pipe is determined using the following correlation [11], which shows good agreement with results from CFD simulations [12].

$$f = \frac{d_H}{s}\left\{1 - \left(\frac{d_H}{d_H + 0.438s}\right)^2\right\}^2 \tag{6}$$

where s denotes the corrugation pitch.

Ergun equation [13] is well-known for calculating the pressure drop through a catalyst bed.

$$-\frac{\Delta P}{l} = 150\frac{\left(1-\varepsilon_p\right)^2}{{\varepsilon_p}^3}\frac{\mu}{{d_p}^2}U + 1.75\frac{\left(1-\varepsilon_p\right)}{{\varepsilon_p}^3}\frac{\rho}{d_p}U^2 \tag{7}$$

where l is the catalyst bed length, ε_p is the porosity, d_p is the particle diameter, μ is the fluid viscosity and U is the superficial fluid velocity.

Tatsumoto et al. [12] reported that a pressure drop through complex-shaped equipment, such as the heater, the heat exchanger, the accumulator, and the moderators is expressed as follows.

$$\Delta P = F\frac{\dot{m}^2}{\rho} \tag{8}$$

where F is the geometry parameter, which is determined based on CFD results [12].

2.2.4 Forced flow heat transfer

Tatsumoto et al. [14] developed an experimental system to measure heat transfer characteristics in the forced flow of liquid and supercritical hydrogen. They reported that the forced flow heat transfer in a single phase could be predicted using the Dittus-Boelter correlation [15].

$$Nu = 0.023Re^{0.8}Pr^{0.4} \tag{9}$$

where Nu is the Nusselt number and Pr is the Prandtl number.

2.2.5 Radiation flow heat transfer

The heat inleak is calculated according to the following correlation, in which an equivalent thermal conductivity, λ_e [16], was modified as follows:

$$\lambda_e = A\left(3.65\times10^{-13}n^2\left(\frac{T_h+T_c}{2}\right) + 1.1\times10^{-13}\frac{(T_h+T_c)\left({T_h}^2+{T_c}^2\right)}{n}\right) \tag{10}$$

IOP Conf. Series: Materials Science and Engineering **1344** (2026) 012065 doi:10.1088/1757-899X/1344/1/012065

where the symbols h and c represent hot and cold, respectively, n is the number of layers of the wrapped MLI (multi-layer insulation) and A is an empirical factor determined to be 5000 based on measured data.

2.2.6 Heat exchanger
The heat exchanger, with a length of 0.69 m, consists of 11 layers for helium stream and 10 layers for hydrogen stream. The heat transfer coefficient of the heat exchanger, h_c, was calculated using Colburn j-factor, j_H.

$$j_H = \frac{h_c}{GC_p} Pr^{2/3} \tag{11}$$

where G is the mass flow rate per unit cross-section area, C_p is the specific capacity, and $j_H = 0.555(Re + 500)^{-0.482}$ for herringbone fins [17].

2.2.7 PID control of heater power
The power of the orifice type heater is regulated by a PI (proportional-integral) control system to maintain the outlet temperature at 20.95 K.

$$u(t) = K_p \left(e + \frac{1}{T_I} \int e\, dt\right) \tag{12}$$

where $u(t)$ is the output of the PID controller, K_p is the proportional gain, e is the error, and T_I is the integral time.

2.2.8 Simulation procedure
The enthalpy equation is solved using the finite volume method, in which the convection term is discretized with a central differencing scheme, and the diffusion term is neglected to simplify the calculation. Time integration is performed explicitly with a time step (Δt) of 5 ms for the overall system, while a finer time step of 0.2 ms is used for the heat exchanger. This smaller time step ensures more accurate and stable calculations for the heat exchanger, while the larger time step helps reduce the overall computational time efficiently. The thermophysical properties of hydrogen are expressed as polynomial functions of temperature and pressure, obtained through least-square fitting of the values calculated by GASPAK [17], with a fitting error within 1.0%.

As initial conditions, the hydrogen and helium pressures in the bellow are set to 1.5 MPa and 1.55 MPa, respectively. The pump speed is set to 40,000 rpm. As boundary conditions at the cold end of the heat exchanger, the helium supply temperature, pressure, and flow rate are set to 16.5 K, 1.652 MPa, and 0.27 kg/s, respectively.

The discharge flow rate is determined based on the overall pressure drop and the pump performance. Initially, the pressure drop is estimated using a tentative flow rate. The actual pressure drop and flow rate are obtained through an iterative solution process. The flow rates in the parallel distribution lines are adjusted iteratively until the pressure drop in each line becomes uniform. The pressure drop through each component is calculated using eqs. (5) to (8). This process is repeated until the difference between the overall pressure drop in the hydrogen loop and the pump head as defined by the pump characteristics converge to less than 10^{-3}.

The heat transfer between the pipe and hydrogen is calculated using equations (9). Heat inleaks from the MLI, spacers, and supports are incorporated as an energy source in equation (4), which is used to solve heat transport across the CMS loop. The propagation of temperature fluctuations through the heat exchanger is evaluated using the heat exchanger model described in [8]. The heater power is regulated by a PI control system to maintain the outlet temperature at 20.95 K. Finally, the enthalpy in each grid cell is converted into a representative temperature. A non-linear filter method [18] is applied to the conversion to the temperature distribution to ensure numerical stability.

Finally, the volume change of the bellows in the accumulator and the associated pressure fluctuations are calculated based on the temperature distribution at each time step. Initially, the helium pressure is determined iteratively using an assumed bellows volume change, ensuring that the helium mass remains consistent between the current and previous time steps. Subsequently, the hydrogen pressure is calculated from the temperature distribution to satisfy the mass conservation. The expansion and contraction of the bellows are driven by the pressure difference between the hydrogen and the helium [4], which depends on its spring constant. These calculations are repeated iteratively until the pressure difference, P2-P1, matches the driving force defined by the bellows' spring constant.

3. Results and discussion

Figure 3 presents the validation results of the heat exchanger model described in Section 2.2.6, using the helium temperature at the warm end (T11) and the hydrogen temperature at the cold end (T01) during the cooldown operation. The calculation utilized the feed helium temperature (T12), hydrogen return temperature (T07), and flow rates as boundary conditions. The calculated temperatures of helium (T11) and hydrogen (T01) at the heat exchanger were in good agreement with the measured values [2], with deviation of less than 2% and 1%, respectively.

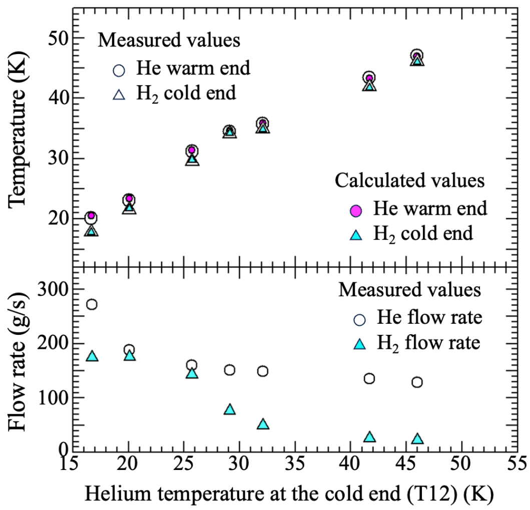

Figure 3. Verification results of the heat exchanger model.

Figure 4 shows the simulation results of the temperature distributions across the CMS loop under steady-state conditions, where the pump speed was 40,000 rpm, CV200 to 58%, CV300 to 60% and CV400 to 100%, consistent with the measurement conditions [12]. The boundary conditions included a feed helium temperature (T12) of 16.52 K and a helium flow rate ($\dot{m}_{He}$) of 0.271 kg/s. The calculated total circulation flow rate ($\dot{m}_T$) was 181.8 g/s, and the calculated distribution flow rates to the decoupled, poisoned and coupled moderators $\dot{m}_D$, $\dot{m}_P$, and $\dot{m}_C$ were 55.4 g/s, 57.5 g/s, and 69.0 g/s, respectively. These calculated flow rates were within 4% of the measured values shown in parentheses in the figure. The calculated hydrogen temperature at the cold end (T01) and warm ends (T07) of the HX were 17.9 K and 21.3 K, respectively. The temperature distributions obtained from the simulation

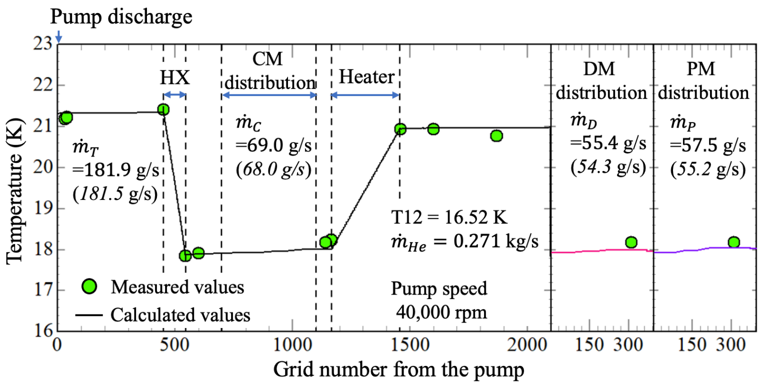

Figure 4. Steady-state temperature distribution across the CMS loop.

closely matched the measured values at each location. These results confirmed that the developed simulation code accurately reproduces both the temperature distributions and flow rates in the CMS loop.

Figure 5 shows the simulation results of the flow distributions at a pump rotational speed of 40,000 rpm. In this simulation, the valve position of CV400 was fixed at 100%, while the valve positions of CV200 and CV300 were varied from 100% to 25%. As the positions of CV200 and CV300 decreased, the pump head increased, resulting in a reduction of the total flow rate. Although the flow rates to the DM and PM decreased, the flow rate to the CM increased. These trends were consistent with the measured pump head and flow rates [12]. The nuclear heating in the CM is estimated to be approximately twice that in the DM and PM. Consequently, the flow rate required for the CM is also twice that of the DM and PM. Therefore, adjusting the valve positions of CV200 and CV300 is an essential and effective approach to increase the CM flow rate for higher proton beam operations. Under the conditions of CV200 = 40%, CV300 = 40%, and CV400 = 100%, the CM flow rate reaches 83 g/s, which satisfies the requirement for 1-MW proton beam operation and is approximately twice the DM and PM flow rate of 38.0 g/s.

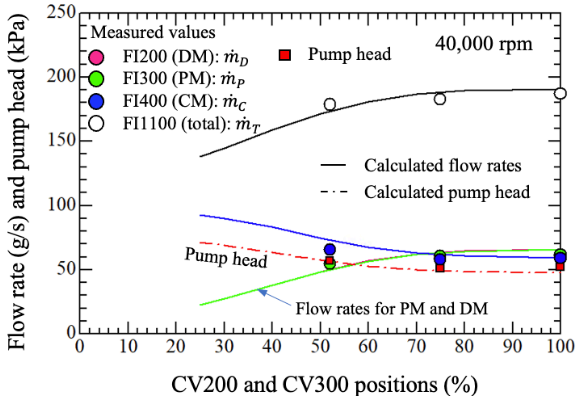

Figure 5. Simulated flow distributions.

Figure 6 shows the simulated propagation of temperature fluctuations throughout the CMS loop following a sudden decrease in heater power by 2720 W for 20 seconds, under the same experimental conditions [19]. The applied boundary conditions included a feed helium temperature (T12) of 17.68 K and a feed helium flow rate ($\dot{m}_{He}$) of 282.6 g/s. The calculated hydrogen supply temperature (T01) was 18.77 K, and the circulation flow rate ($\dot{m}_T$) was 190.1 g/s. In the J-PARC CMS, only the heater power setpoints were defined, and the actual heater powers were not measured. Therefore, in this simulation, the ramping rates and response time were adjusted to match the observed temperature fluctuations at the heater outlet (T03), considering the effects of heat capacity and control delay. The heater power ramped

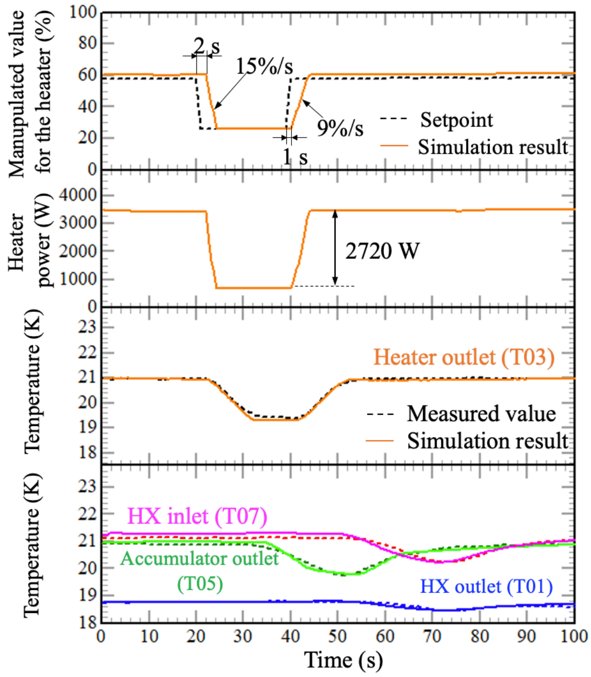

(a) Heater power and Temperatures

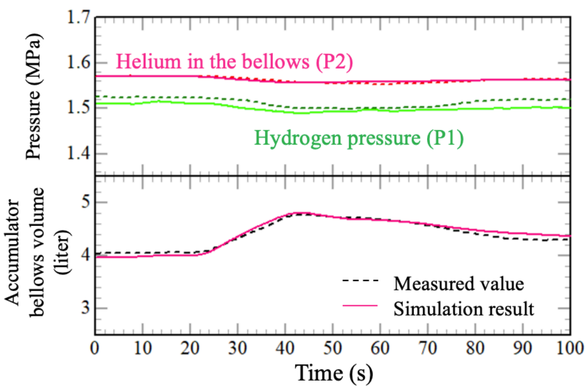

(b) Pressure and accumulator

Figure 6. Propagation of temperature and pressure fluctuations by a sudden decrease in heater power.

down at 1200 W/s with a 2 second delay and ramp up at 700 W/s with a 1 second delay. As a result, the heater outlet temperature decreased by 1.64 K. The temperature fluctuations propagated downstream of the heater following the flow direction and gradually mitigated by the catalyst vessel and heat exchanger. These components effectively dampened the fluctuation in the supply temperature (T01), reducing it to 0.32 K. The simulation results demonstrated that the developed code accurately reproduced the propagation behaviors of temperature fluctuations within the CMS loop. Additionally, it successfully predicted the associated change in hydrogen and helium pressures and the corresponding volume variation of the bellows.

4. Conclusions

A comprehensive simulation code was developed to predict the propagation of temperature fluctuations throughout the entire CMS loop, including the resulting temperature variations in the helium flow returning to the refrigerator cold box. The accuracy of the simulation was validated by comparing the calculated temperature distributions and flow rates under steady-state conditions (1.5 MPa and 17.9 K) with experimental data obtained under the same conditions. In addition, the simulation accurately reproduced the propagation behaviors of temperature fluctuations induced by rapid changes in heater power. The developed simulation code has proven to be a valuable tool for optimizing the operational conditions of the J-PARC CMS.

Acknowledgments
This paper is supported by the Swedish Research Council, and European Spallation Source ERIC under The SAKURA Mobility Programme.

References

[1] Oyama Y, "Present Status of J-PARC High Intensity Proton Accelerator Project in Japan," in The Proceedings of ICANS-XVI, edited by G. Mank and H. Conrad, ISSN 1433-559X, ESS 03-136-M1, Forschungszentrum Jülich GmbH, Jülich, Germany, 2003, pp. 7-11
[2] Tatsumoto H, Aso T, Ohtsu K, Uehara T, Sakurayama H, Kawakami Y, Kato T and Futakawa M 2010 in *Advances in Cryogenic Engineering* **55A** pp 297-304
[3] Tatsumoto H, Aso T, Kato T, Ohtsu K, Hasegawa S, Maekawa F, Futakawa M, Proceedings of ICEC 22 and ICMC 2008, edited by Ho-Myung CHANG, et al., The Korea Institute of Applied Superconductivity and Cryogenics, Korea, 2008, pp. 711-716.
[4] Tatsumoto H, Aso T, Ohtsu K and Kawakami Y 2015 *Physics Procedia* **67** 123-128.
[5] Tatsumoto H, Aso T, Kato T, Ohtsu K, Maekawa F and Futakawa M 2011 *Cryogenics* **51** 315- 320.
[6] Tatsumoto H, Aso T, Ohtsu K, Kato T, and Futakawa M 2010 in *Advances in Cryogenic Engineering* **55B** 1154-1161
[7] Tatsumoto H, Horvath, Arnold P. and Boros M., 2024 IOP Conf. Ser: Mater Sci Eng 1301 13011073
[8] Tatsumoto H, Horvath, Arnold P. and Boros M., 2024 IOP Conf. Ser: Mater Sci Eng (ICEC24-HX)
[9] Tatsumoto H, Aso T, Ohtsu K, Uehara T, Sakurayama H, Kawakami Y, Kato T, Futakawa M and Yoshinaga S 2011 *Proc. of 23th ICEC-ICMC 2010* pp 377-38
[10] Colebrook C.F. *J. Inst. Civ. Eng* 11 (1938) 133
[11] *Kanro Duct no Ryutaiteiko* 1979 (The Japan Society of Mechanical Engineers) p.33. (in Japanese)
[12] Tatsumoto H, Aso T, Ohtsu K, Kato T, and Futakawa M *IOP Conf. Ser: Materials Science and Engineering* **101** (2015) 012109
[13] S. Ergun, 1952. Fluid flow through packed columns. Chem. Eng. Prog., 48, 89-94
[14] Tatsumoto H, Shirai Y, Shiotsu M, Hata K, Kobayashi H, Naruo Y and Inatani Y 2010 J.Phys:Conf. Seri. 234, 032056
[15] Van Sciver S W 1986 Helium Cryogenics (New York: Plenum Press) p 251
[16] Barron, Randall F 1985 *Cryogenic Systems 2nd edition* North Carolina USA Oxford University.
[17] GASPAK user's guide 1998 (Cryodata)
[18] Shyy, W, Chen, MH., Mittal, R., Udaykumar, HS., J Comput Phys, 102, p.49 (1992)
[19] Tatsumoto H, Ohtsu K, Aso T, Kawakami Y, and Teshigawara M 2014 in *Advances in Cryogenic Engineering* **1573** 66-73.